ORIGINAL RESEARCH PAPER

Medical Science

FORCE FIELD, INTERNAL COORDINATES AND VIBRATIONAL STUDY OF ALKALOID TROPANE HYDROCHLORIDE BY USING THEIR INFRARED SPECTRUM AND DFT CALCULATIONS

KEY WORDS: Tropane hydrochloride, vibrational spectra, molecular structure, solvation energy, DFT calculations

Roxana A. Rudyk Cátedra de Química General, Instituto de Química Inorgánica, Facultad de Bioquímica. Química y Farmacia, Universidad Nacional de Tucumán, Ayacucho 471, (4000) San Miguel de Tucumán, Tucumán, Argentina.

Silvia Antonia Brandán Cátedra de Química General, Instituto de Química Inorgánica, Facultad de Bioquímica. Química y Farmacia, Universidad Nacional de Tucumán, Ayacucho 471, (4000) San Miguel de Tucumán, Tucumán, Argentina.

ABSTRACT

In this work, the complete vibrational assignments of cationic, neutral and hydrochloride species of alkaloid tropane and their force fields were studied in gas and aqueous solution phases by using the experimental available FT-IR spectrum of tropane hydrochloride in the solid state and hybrid calculations derived from the density functional theory (DFT). The normal internal coordinates for all species were employed to compute the corresponding force fields and force constants by using the scaled quantum mechanical force field (SQMFF) methodology at the B3LYP/6-31G* level of theory. In the vibrational analyses, the normal internal coordinates corresponding to rings of six and five members were employed for the bicyclic (N-methyl-8-a-zabicyclo[3.2.10]octane) group because it can be considered as formed by two fused piperidine and pyrrolidine rings, respectively. Here, the redundant internal coordinates due to the C-N-C group shared by both rings was identified and then, removed. This way, the complete assignments of the 66, 69 and 72 vibration normal modes expected for the neutral, cationic and hydrochloride tropane species respectively are reported for first time. Here, the very good agreement that exist between the predicted IR spectrum for the cationic form with the corresponding experimental one for tropane hydrochloride reveals that in the solid state tropane hydrochloride is as cationic, as expected because it is a salt. In addition, the structures optimized for the cationic and hydrochloride species confirm the fast N-methyl inversion in gas phase and in aqueous solution at room temperature, as was reported in the literature.

INTRODUCTION

The alkaloid tropane hydrochloride, whose IUPAC name is 8-Azabicyclo[3.2.1]octane, n-methyl- hydrochloride present a bicyclic (N-methyl-8-a-zabicyclo[3.2.10]octane) group in their structure with a tertiary nitrogen atom which confers to all the tropyl alkaloids and their derivatives remarkable pharmacological and medicinal properties [1-27]. From the pharmacological point of view the most important tropyl alkaloids are scopolamine, cocaine and atropine being tropane the most simple, as mentioned by Gyermek [28]. In the literature there are many studies related with the biological activities of those alkaloids or with their detection by using high-performance liquid chromatography, NMR spectroscopy or other techniques [4,7-9,16,18,22,24] but few studies are reported on the infrared and Raman spectra and their corresponding assignments [8,25]. So far, none of the aforementioned alkaloids, including the tropane, were studied from the vibrational point of view probably due to that the presence of that bicyclic ring in its structures makes it difficult to assign the observed bands. The constructions of the normal internal coordinates of that ring are not simple due to the existence of two fused piperidine and pyrrolidine rings sharing a common C-N-C group [28]. This bicyclic ring with a tertiary nitrogen atom confers to all tropane alkaloids anticholinergic activities, as reported by Pauling and Datta [23]. The vibrational studies of these alkaloids are of interest to their detection especially because the tropane derivatives undergo fast N-methyl inversion in aqueous and methanol solutions at room and low temperature, as reported by Lazny et al. by using NMR spectroscopy and DFT calculations [24]. Hence, the vibrational spectroscopy is a quick, easy and useful technique to their identifications taking into account the importance of these alkaloids for the human health. Our aims in this work are: (i) to study theoretically the alkaloid tropane in its neutral, cationic and hydrochloride forms by using DFT calculations in gas and aqueous solution phases and, (ii) to perform the complete assignments of those three species by using the experimental available FT-IR spectrum of tropane hydrochloride, their corresponding normal internal coordinates and the force fields computed with the SQMFF procedure [29]. Here, the structures of those three tropane species in both media were first optimized by using the hybrid B3LYP/6-31G* method [30,31] and, then, their corresponding force fields were performed at the same level of theory with the SQMFF methodology. Whereas the normal internal coordinates for the bicyclic group were built knowing that the (N-methyl-8-a-zabicyclo[3.2.10]octane) group is constituted by two fused piperidine and pyrrolidine rings, as mentioned by Gyermek [28], both of six and five members, respectively where the redundant internal coordinates corresponding to the C-N-C group common shared by both rings was first identified and, then, removed. In addition, the force constants were also reported for all those species in both media and, latter compared with other reported for cyclic nitrogen compounds with different properties [32]. The methodology employed here for the alkaloid tropane and their coordinates, later, will be used in a future to perform the force fields for other alkaloids, such as scopolamine or atropine.

COMPUTATIONAL INFORMATION

In this work, the GaussView [33] and Gaussian 09 programs [34] were used to model and optimize the three neutral, cationic and hydrochloride tropane structures in gas and aqueous solution phases using the hybrid B3LYP/6-31G* method [30,31]. It is necessary to clarify that structurally, for the piperidine ring according their potential energy surface are expected various conformations which are, half-chair, boat, twist-boat or chair, being the most stable and abundant the chair form, as mentioned by Gyermek [28] and, as experimentally were reported for other tropane alkaloids by using X-ray diffraction [35,36] and vibrational circular dichroism [37]. For these reasons, all structures of those tropane species were optimized with the piperidine ring in chair conformation. The theoretical structures can be seen in **Figure 1** while the identifications of the two fused piperidine and pyrrolidine rings belong to the (N-methyl-8-a-zabicyclo [3.2.10]octane) group, both of six (R1) and five members (R2), respectively is shown in **Figure 2.**

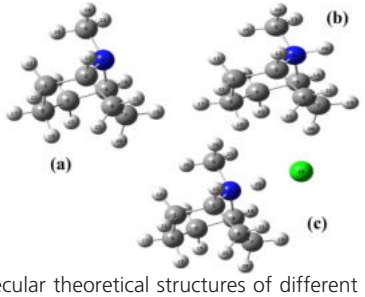

Figure 1: Molecular theoretical structures of different species of alkaloid tropane: a) neutral, b) cationic and, c) hydrochloride and

the atoms numbering.

The studies of those species in solution were carried out with the self-consistent reaction field (SCRF) method and the integral equation formalism variant polarised continuum (IEFPCM) model at the same level of theory [38,39] because both methods consider the solvent effects. On the other hand, the solvation model (PCM/SMD) [40] was employed to compute the solvation energies of those species while the volumes variations involved in the solvation process were computed with the Moldraw program [41] at the same level of theory. Furthermore, the force fields were calculated by using the SQMFF approach [29] and the Molvib program [42] while the normal internal coordinates for the three species were similar to those reported by Pulay et al [43] for six and five member's rings. Here, the coordinate corresponding to one of the three deformation ring for the six members ring was removed because the C-N-C group is shared by both rings. Subsequently, the calculated force fields for those three tropane species in both media and at the same theory level were used to perform their complete assignments by using the Potential Energy Distribution (PED) 10%. Later, the force constants in both media were also calculated from their corresponding force fields transformed from Cartesian coordinates to normal internal which were later compared with those cyclic nitrogen species structurally associated to the tricyclic bisguanidine compound and to the toxic agent, saxitoxin [32].

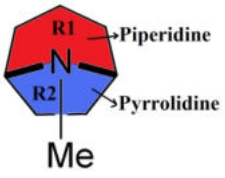

Figure 2: The bicyclic (N-methyl-8-a-zabicyclo[3.2.10]octane) group common to all alkaloids tropane and the identifications of both fused rings, piperidine and pyrrolidine where R1 correspond to the six members and R2 to the five members.

RESULTS AND DISCUSSIONDIPOLE MOMENTS AND SOLVATION ENERGIES

For the neutral, cationic and hydrochloride tropane forms, the total energies, dipole moments, volume variation and solvation energy were calculated in gas and aqueous solution phases by using the hybrid B3LYP/6-31G* method. The results can be seen in **Table 1.**

TABLE – 1

Calculated total energies (E), dipole moments (μ), volume variations (V) and solvation energies (G) for the neutral, cationic and hydrochloride tropane forms in gas and aqueous solution phases.

B3LYP/6-31G*				
Gas phase				
Species	E (Hartrees)	μ (D)	V (Å3)	
Neutral	-368.6284	0.76	154.3	
Cation	-369.0200	2.96	161.3	
H-Cl	-829.4529	9.43	182.7	
PCM				
	E (Hartrees)	μ (D)	V (Å3)	V (Å3)
Neutral	-368.6324	1.39	154.8	0.5
Cation	-369.1070	4.26	159.8	-1.5
H-Cl	-829.4824	13.96	182.8	0.1
Solvation energy (kJ/mol)				
	Gu#	Gne	Gc	
Neutral	-10.49	0.75	-11.24	
Cation	-228.21	15.34	-243.55	
H-Cl	-77.38	15.05	-92.43	

Analyzing exhaustively the values we observed that the hydrochloride species in both media present the higher dipole moment and volume values but that species has the lowest volume variation in solution while the cationic form present the higher volume contraction in solution, as expected because this ionic species is highly hydrated in solution due to their higher solvation energy. Here, the uncorrected solvation energy was calculated as the difference between the total energies in aqueous solutions and the values in gas phase while the corrected values are defined as the difference between the uncorrected and the total non-electrostatic solvation energies where the total non electrostatic terms due to the cavitation, dispersion and repulsion energies are computed with the SMD model [40]. The volume values calculated for the three tropane species are in satisfactory agreement with the value of 142 Ĺ3 mentioned by Gyermek [28]. Obviously, the hydrochloride form is the more voluminous compound in both media due to the Cl atom present in their structures. On the contrary, the neutral species has the lower solvation energy values in correlation with their low dipole moment values in both media. Note that the dipole moment values for all the species increase slightly in solution due to the solvation.

STRUCTURAL STUDY IN GAS PHASE AND IN AQUEOUS SOLUTION

The calculated geometrical parameters for the neutral, cationic and hydrochloride tropane forms in gas and aqueous solution phases are presented in Table 2 compared with the corresponding experimental values reported for the two compounds that contain the bicyclic (N-methyl-8-a-zabicyclo[3.2.10]octane) group, 3α-Bromotropane Hydrobromide Monohydrate (BHM) [35] and *6β,7β-Epoxy-IαH*,5αH~tropan-3α-yl(-)-2,3-Dihydroxy-2-phenylpropionate from its n-Butylbromide [36].

In **Figure 3** it is compared the stereoscopic view of the experimental structure of cation BHM with those optimized for the neutral, cationic and hydrochloride tropane forms. Note that the neutral form is optimized with the N-CH3·group in the same equatorial position than that experimental structure but the other cationic and hydrochloride forms of tropane were here optimized with the N-CH3·group in inverted axial position, as observed in Figure 3 and, as suggested by Lazny et al. by using NMR spectroscopy and DFT calculations [24]. This preference is related probably to that there are lower interactions when the distances with the H atoms are higher or in some cases to the formation of H bonds, as reported by Muńoz el al for the (2)-(3S,6S)-3a,6b-Diaceto xytropane derivative [37]. On the other hand, we should take into account that in the calculations the molecule is free while in the solid state the interactions due to the forces of crystalline packing are important. The theoretical and experimental parameters for the three species are compared in Table 2 by using the root mean square deviation (RMSD) values. In this table, only some distances and bond angles are reported because the three structures are practically symmetrical, as observed by the same N-C and C-C bonds that present the six and five member's rings. Hence, we observed that the better bond lengths and angles are obtained when those parameters are compared with the n-Butylbromide structure. Notice that for the hydrochloride species in aqueous solution the same rmsd values are obtained for the bond lengths (0.016 Ĺ) and angles (2.8ş), respectively. In general, the parameters of the neutral and hydrochloride species increase in solution but, in particular, for the cationic structure we observed the decreasing in the C-C, N-C and N-CH_3 distances and bond angles as a consequence of their volume contraction in this medium. In relation to the dihedral angles, we observed that the neutral species is different from the cationic and hydrochloride structures due principally to their C-C-N-CH_3 and C-C-N-CH_3 dihedral angles corresponding to the six (A6) and five (A5) member's rings. Later, these differences could justify that the optimized structures for the neutral species are different from those predicted for the cationic and hydrochloride forms, as observed in Figure 3.

VIBRATIONAL STUDY

The neutral, cationic and hydrochloride tropane structures in both media were optimized by B3LYP/6-31G* calculations with C1 symmetries. Here, for the neutral, cationic and hydrochloride tropane species are expected 66, 69 and 72 vibration normal

modes, respectively where all modes present activities in the infrared and Raman spectra. The infrared spectrum of tropane hydrochloride in the solid phase and recorded in the 4000-680 cm-1 region was taken from that experimental available from Ref [44] and the comparisons with the corresponding predicted by B3LYP/6-31G** calculations for the neutral, cationic and hydrochloride forms in gas phase can be seen in Figure 4.

TABLE – 2

Comparison of calculated geometrical parameters for the neutral, cationic and hydrochloride tropane forms in gas and aqueous solution phases compared with experimental ones for tropane derivatives

Parameters	B3LYP/6-31G*a						Exp[b]	Exp[c]
	Neutral		Cationic		Hydrochloride			
	Gas	PCM	Gas	PCM	Gas	PCM		
Bond lengths (Å)								
N-CH[3]	1.458	1.467	1.496	1.491	1.478	1.486	1.520(4)	1.520
N-C	1.478	1.487	1.539	1.528	1.507	1.521	1.450(4)	1.530
N-C	1.478	1.487	1.539	1.528	1.508	1.521	1.580(4)	1.530
C-C(A5)	1.560	1.556	1.542	1.541	1.544	1.542	1.490(5)	1.520
C-C(A5)	1.560	1.556	1.542	1.541	1.544	1.542	1.600(4)	1.520
C-C(A6)	1.539	1.538	1.533	1.531	1.535	1.532	1.580(4)	1.540
C-C(A6)	1.540	1.540	1.541	1.541	1.543	1.542	1.520(4)	1.540
C-C(A6)	1.540	1.540	1.541	1.541	1.543	1.542	1.460(4)	1.540
C-C(A6)	1.539	1.538	1.533	1.531	1.535	1.532	1.460(4)	1.540
RMSD I	0.063	0.061	0.058	0.058	0.059	0.016		
RMSD II	0.037	0.032	0.014	0.015	0.021	0.016		
Bond angles (°)								
C-N-C	113.5	111.8	118.0	117.7	118.2	117.6	108.0(3)	113.0
C-N-C	113.5	111.8	118.0	117.7	118.2	117.6	112.0(2)	112.0
C-N-C(A5,A6)	101.6	100.8	101.6	102.0	102.6	102.1	101.0(2)	101.0
N-C-C(A5)	105.2	105.3	100.4	100.6	100.5	100.7	103.0(3)	104.0
C-C-C(A5)	103.6	103.7	105.4	105.3	104.9	105.1	105.0(3)	107.0
N-C-C(A6)	107.2	107.8	109.0	108.9	109.8	109.4	104.0(3)	109.0
C-C-C(A6)	111.0	111.2	111.9	111.9	111.5	111.7	117.0(3)	113.0
RMSD I	3.1	2.8	4.6	4.5	4.9	2.8		
RMSD II	1.6	1.4	2.9	2.8	3.1	2.8		
Dihedral angles (°)								
C-C-N-CH3(A6)	-161.6	-165.5	-59.8	-59.5	-61.8	-59.7		
C-C-N-CH3(A5)	78.6	75.0	179.7	179.3	178.4	179.3		
C-C-C-C	-54.3	-54.5	-51.3	-51.7	-52.5	-52.1		

aThis work, bRef [35] for 3α-Bromotropane Hydrobromide Monohydrate, cRef 36] for *6β,7β-Epoxy-IaH,5aH~tropan*-3α-yl(-)-2,3-Dihydroxy-2-phenylpropionate from its n-Butylbromide; A6, six member's ring; A5, five member's ring..

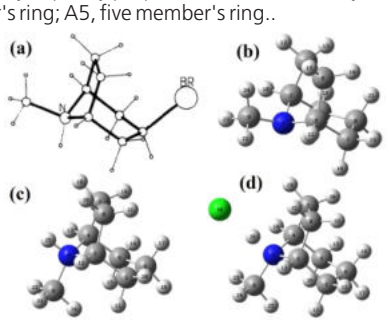

Figure 3: Comparison among the stereoscopic view of the experimental structure of cation 3α-Bromotropane Hydrobromide Monohydrate [35] with those optimized for the neutral, cationic and hydrochloride tropane forms.

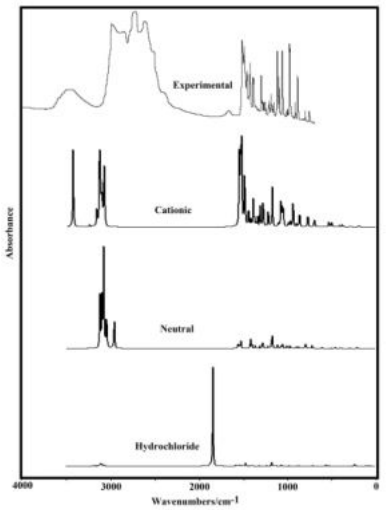

Figure 4: Comparisons between the experimental FTIR spectrum of tropane hydrochloride in the solid state with the corresponding predicted for their neutral, cationic and hydrochloride species in the gas phase at B3LYP/6-31G** level of theory.

We observed a very good correlation between the spectra predicted for the cationic form and the corresponding experimental one, as expected because it is clear that the solid sample is a chloride salt. The predicted Raman spectra for all the species were first converted from scattering activities to relative Raman intensities and, these new spectra are shown in **Figure 5.** These corrections were performed considering a laser excitation frequency of 634 nm by using that equation reported in the literature [45,46]. The observed and calculated wavenumbers together with the corresponding assignments for the neutral, cationic and hydrochloride tropane forms can be seen in **Table 3**. The complete assignments for the three tropane species were performed by using their normal internal coordinates and force fields calculated in both media with the SQMFF methodology [29] and the Molvib program [42]. Here, the definitions of natural internal coordinates are presented in Table 4 only for the tropane hydrocloride species because it has higher vibration modes. For the cationic species it is necessary to remove those coordinates related to the H-Cl group while for the neutral species the coordinated related to N-H group should be removed. Besides, only those PED contributions 10 % were considered to perform the assignments of the observed bands to the normal vibration modes. In this study, we have used those scale factors calculated by Rauhut and Pulay [29] using the 6-31G* basis set. Furthermore, a short discussion of the assignments for some groups is presented at continuation.

Band Assignments

NH modes. Obviously, these modes are only expected for the cationic and hydrochloride species. For instance, in the anti-hypertensive clonidine hydrochloride the N-H stretching mode is assigned to 3427 cm-1 and in the monomer neutral this mode is observed at 1711 cm-1 [47], in nitrogen species derived from tricyclic bisguanidine compound these modes are assigned at 3403 and 3397 cm-1 [32] while in N-benzylamides [48] and other compounds containing this stretching modes are assigned between 3480 and 3254 cm-1 [49-51]. Hence, the IR band of medium intensity at 3419 cm-1 is easily assigned to that mode for the cationic species while for the hydrochloride species is assigned to the weak band at 1626 cm-1 because in this species that mode is predicted at 1760 cm-1, as indicated in **Table 3.** Here, the broad band at 3419 cm-1 is typical of inter-molecular N–H···N bonds, as reported for compounds containing N-H groups [32,47,48]. The in-plane deformation modes for the cationic and hydrochloride species are predicted coupled with other modes between 1532

and 1277 cm-1 while in N-benzylamides [48] are observed between 1508 and 1513 cm-1; hence, the bands between 1626 and 1393 cm-1 are assigned to those vibration modes. Here, it is necessary to explain that in both cationic and hydrochloride species the N atom has sp3 hybridization and, for this reason, the constructions of the normal internal coordinates for the N-H group in that case is tetrahedral and different from those species containing the N atom with sp2 hybridization [47-51] because in this case the group N-H is planar. Later, there are not out-of-plane deformation modes in the cationic and hydrochloride species.

CH modes. In the three neutral, cationic and hydrochloride species are expected only the C-H stretching and rocking modes because the C atom present sp3 hybridization, in form similar to the N-H groups. Hence, the C-H stretching modes are assigned between 2996 and 2985 cm-1 because the SQM calculations predicted these modes for the three species in that region while the group of bands between 1351 and 1219 cm-1 can be easily assigned to the rocking modes for the three species, as detailed in **Table 3**.

Ch3 modes. Nine normal vibration modes are expected for each neutral, cationic and hydrochloride tropane species because they have a CH3 group in their structures. Hence, three antisymmetric and symmetric stretching modes, three antisymmetric and symmetric deformation modes, two rocking modes and one twisting mode are expected. **Table 3** shows clearly that in the three species the stretching modes are calculated as practically pure modes between 3098 and 2966 cm-1 where in the cationic species is predicted at higher wavenumbers than the other ones while the deformation modes are predicted

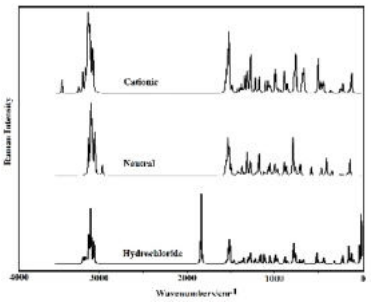

Figure 5. Comparisons between the predicted Raman spectra of neutral, cationic and hydrochloride tropane species in the gas phase at B3LYP/6-31G** level of theory.

TABLE – 3 Observed and calculated wavenumbers (cm-1) and assignments for the neutral, cationic and hydrochloride tropane forms

Exp[c]	B3LYP/6-31G* Method[a]					
	Hydrochloride		Cationic		Neutral	
IR	SQM[b]	Assignments[b]	SQM[b]	Assignments[b]	SQM[b]	Assignments[b]
3419m			3280	N3-H25		
			3098	aCH_3		
	3054	aCH_3	3054	aCH_3		
	3041	aCH_3				
	3023	aCH_2(C7)	3024	aCH_2(C7)		
3014sh	3011	aCH_2(C8)	3011	aCH_2(C8)		
			2997	aCH_2(C6)		
			2996	C2-H12		
			2994	C4-H13		
	2988	C4-H14	2984	aCH_2(C5)	2986	aCH_3
	2985	C2-H13	2984	aCH_2(C1)	2986	aCH_2(C4)
	2977	aCH_2(C6)	2977	sCH_3		
	2966	sCH_3				
	2966	sCH_2(C7)	2971	sCH_2(C8)	2967	aCH_2(C5)
2960sh	2965	sCH_2(C5)			2966	aCH_2(C7)
	2961	aCH_2(C1)	2964	sCH_2(C7)	2957	sCH(C2,C3)
	2959	sCH_2(C8)			2957	aCH_2(C6)
			2949	sCH_2(C1)	2948	aCH(C2,C3)
2947vs			2948	sCH_2(C5)	2947	aCH_3
			2942	sCH_2(C6)	2945	aCH_2(C8)
					2941	sCH_2(C4)
2930vs	2932	sCH_2(C6)			2935	sCH_2(C5)
	2929	sCH_2(C5)			2918	sCH_2(C6)
	2929	sCH_2(C1)			2915	sCH_2(C7)
					2911	sCH_2(C8)
2805vs					2834	sCH_3
2684vs		1393+1266=2659		1426+1266=2692		
2576s		1482+1086=2568				
1626w	1760	N3-H26				
1608sh	1532	ρN3-H26				
1482vs			1485	δCH_2(C8)	1481	δCH_2(C4), δCH_2(C5)
1476vs	1477	δaCH_3	1478	δaCH_3		
1476vs	1475	δCH_2(C1), δCH_2(C5)	1475	δaCH_3, ρN_3-H25	1475	δaCH_3
1459sh	1461	δCH_2(C8)	1461	δCH_2(C5)	1466	δCH_2(C8)
1455s			1459	δCH_2(C8)	1454	δaCH_3
1455s	1453	δCH_2(C6)	1451	δCH_2(C6)	1453	δCH_2(C4), δCH_2(C5)
1449sh	1448	δaCH_3, δCH_2(C1)			1447	δCH_2(C7)
1443sh	1445	δaCH_3	1446	δCH_2(C1)		
1443sh	1442	δCH_2(C7)	1434	δaCH_3, ρN3-H25	1439	δCH_2(C6)

1426$_s$	1416	ρ'N_3-H26, N_3-H26	1412	δsCH_3	1420	δsCH^3
1393$_s$	1400	δ$_s$$CH_3$	1402	ρ'N_3-H25 ρC2-H12		
1382sh	1379	wagCH_2(C6)	1385	wagCH_2(C5), wagCH_2(C1)	1377	wagCH_2(C6) wagCH_2(C7)
1382sh	1377	wagCH_2(C5), wagCH_2(C1)	1383	wagCH_2(C1), wagCH_2(C6)	1377	wagCH_2(C8)
1359$_s$	1360	wagCH2(C6), wagCH_2(C5)			1361	wagCH_2(C6) wagCH_2(C7)
1351$_s$	1354	ρ'C_2-H13	1357	wagCH_2(C6)	1359	ρC_3-H11
1351$_s$			1348	ρC4-H13		
1345sh	1343	wagCH_2(C7) wagCH_2(C8)	1342	wagCH_2(C8)		
1328w	1335	wagCH_2(C7)	1334	wagCH_2(C7)	1326	ρ'C3-H11
1324w	1313	ρ'C4-H14, ρC_2-H13			1322	ρ'C2-H10
1299w			1302	ρ'C4-H13	1308	wagCH_2(C4), wagCH^2(C5)
1284vw	1286	ρC4-H14				
1280vw			1277	ρC4-H13, ρ'N3-H25		
1266$_s$	1274	wagCH_2(C8)	1275	ρCH_2(C5), ρCH_2(C1)	1266	ρC2-H10
1266$_s$					1265	ρCH_2(C6), ρCH_2(C7)
1254w	1248	ρCH_2(C8)			1239	R_1(A1), wagCH_2(C4)
1235w	1234	R_1(A1), ρCH_2(C1)	1238	ρCH_2(C7)	1238	ρ'CH_3
1219w			1232	ρ'C2-H12	1229	ρCH_2(C5), ρCH_2(C4)
1185sh	1184	ρCH_2(C7)				
1180w	1183	ρ'CH_3				
1173sh	1173	ρCH_2(C6)	1173	ρCH_2(C6),δCH_2(C8)	1163	ρCH_2(C8)
1154m			1157	ρ'CH_3, ρCH_2(C5)	1156	ρCH_3 ρCH_2(C4)
1149sh	1142	ρCH_2(C5), ρCH_2(C1)	1139	ρ'CH_3	1138	ρCH_3
1132sh			1132	ρCH_3	1134	ρ'CH_3
1128m	1128	ρCH3			1114	N1-C9
1086vs	1085	N3-C9				
1067$_s$	1061	C6-C1	1058	R_1(A1), βR_1(A2)	1071	C6-C8
1067$_s$	1053	R_1(A1)	1056	C6-C5		
1031vs			1029	N3-C9	1043	R^1(A1), βR_1(A2)
1031vs	1006	R_1(A1), R_2(A1)	1000	R_1(A1), R_2(A1)	1011	R_1(A1), R_2(A1)
981w	989	βR_2(A2), βR_1(A2)			998	N1-C2
972w	959	C7-C8, R_2(A21)	967	wCH_2(C7)		
951vs	952	C7-C4, C2-C8	954	C5-C4	954	C2-C6
945vs			952	C7-C4, C2-C8	942	wCH_2(C4), wCH_2(C5)
933sh	928	wCH_2(C7)	916	C7-C8,wCH_2(C6)		
888m	917	C7-C8, wCH_2(C6)	906	βR_2(A2)	919	C2-C4,C3-C5
867sh					913	C4-C5
857$_s$	850	C7-C8	844	C7-C8	840	wCH_2(C8)
831vw	826	C6-C5			818	C7-C8
813w	811	wCH_2(C5), wCH_2(C1)	814	C6-C1	810	wCH_2(C6) wCH_2(C7)
800w			802	wCH_2(C5), wCH_2(C1)		
776m	780	C2-C1C5-C4			784	C3-C7
776m	761	N3-C2	770	C2-C1	750	N1-C3
729m					739	βR_2(A2)
729m			733	N3-C2	731	βR^1(A2)
723sh	716	wCH_2(C8)	714	wCH_2(C8)		
706vw	710	βR_2(A2),βR_1(A2),N3-C4,				
680w	652	wCH_2(C6)	673	N3-C4	675	βR_1(A2), R_1(A1)
			639	wCH_2(C6)		
					563	N1-C9
	535	N3-C9	516	N3-C9		
	502	βR_3(A1)	489	βR_3(A1), βR_1(A2)		
	480	βR_2(A1)	473	βR_2(A1)	484	βR_2(A1)
					434	βR_3(A1)
	380	R_1(A1)	389	R1(A1)		
					372	R1(A1)
	365	R_3(A1)	362	R_3(A1)	366	βN_1-C9
	301	βN_3-C9	300	βN_3-C9	298	R_3(A1)
	285	R_1(A1), R_2(A1)				
			274	R_1(A1), R_2(A1)	268	R_2(A1)
	216	Cl10-H26				
	193	R_2(A1)	195	R_1(A2),wCH_3	205	wCH_3
	192	R_1(A2), R_2(A21)			191	R_2(A1), R_1(A1)
			180	R_2(A1)	185	R_1(A2), R_2(A2)
			170	R_2(A2)		

	151	wCH_3				
	86	δCl10H26N3				
	46	N3-H26, ρ'N3-H26				

Abbreviations: ν, stretching; β, deformation in the plane; γ, deformation out of plane; wag, wagging; τ , torsion; R, deformation ring τ_R, torsion ring; , rocking; w, twisting; δ, deformation; a, antisymmetric; s, symmetric; (A_1), piperidine Ring1; (A_2), pyrrolidine Ring2. [a]This work, [b]From scaled quantum mechanics force field; [c]From Ref [44].

TABLE – 4 Definition of Natural Internal Coordinates for the tropane hydrocloride specie

Modes	Internal coordinate	Definition
S_1	rC-H	C2-H13
S_2	rC-H	C4-H14
S_3	r(C1-H11)-r(C1-H12)	aCH_2(C1)
S_4	r(C1-H11)+r(C1-H12)	aCH_2(C1)
S_5	r(C5-H15)-r(C5-H16)	aCH_2(C5)
S_6	r(C5-H15)+r(C5-H16)	aCH_2(C5)
S_7	r(C6-H17)-r(C6-H18)	aCH_2(C6)
S_8	r(C6-H17)+r(C6-H18)	aCH_2(C6)
S_9	r(C7-H19)-(C7-H20)	aCH_2(C7)
S_{10}	r(C7-H19)+(C7-H20)	aCH_2(C7)
S_{11}	r(C8-H21)-r(C8-H22)	aCH_2(C8)
S_{12}	r(C8-H21)+r(C8-H22)	aCH_2(C8)
S_{13}	2r(C9H25)-r(C9H23)-r(C9H24)	aCH_3
S_{14}	r(C9H23)-r(C9H24)	aCH_3
S_{15}	r(C9H25)+r(C9H23)+r(C9H24)	sCH_3
S_{16}	rN3-H26	N3-H26
S_{17}	rCl10-H26	Cl10-H26
S_{18}	rN3-C2	N3-C2
S_{19}	rN3-C4	N3-C4
S_{20}	rN3-C9	N3-C9
S_{21}	rC2-C1	C2-C1
S_{22}	rC6-C1	C6-C1
S_{23}	rC6-C5	C6-C5
S_{24}	rC2-C8	C2-C8
S_{25}	rC5-C4	C5-C4
S_{26}	rC7-C4	C7-C4
S_{27}	rC7-C8	C7-C8
S_{28}	5 α(H11-C1-H12)+α(C2-C1-C6)	CH_2(C1)
S_{29}	α(H11-C1-C2)+ α(H12-C1-C2)- α(H11-C1-C6)- α(H12-C1-C6)	wag CH_2(C1)
S_{30}	α(H11-C1-C2)+ α(H12-C1-C6)+ α(H11-C1-C6)+ α(H12-C1-C2)	CH_2(C1)
S_{31}	α(H11-C1-C2)+ α(H11-C1-C6)+ α(H12-C1-C2)+ α(H12-C1-C6)	wCH_2(C1)
S_{32}	5 α(H11-C1-H12)+α(C2-C1-C6)	CH_2(C5)
S_{33}	α(H11-C1-C2)+ α(H12-C1-C2)- α(H11-C1-C6)- α(H12-C1-C6)	wag CH_2(C5)
S_{34}	α(H11-C1-C2)+ α(H12-C1-C6)+ α(H11-C1-C6)+ α(H12-C1-C2)	CH_2(C5)
S_{35}	α(H11-C1-C2)+ α(H11-C1-C6)+ α(H12-C1-C2)+ α(H12-C1-C6)	wCH_2(C5)
S_{36}	5 α(H11-C1-H12)+α(C2-C1-C6)	CH_2(C6)
S_{37}	α(H11-C1-C2)+ α(H12-C1-C2)- α(H11-C1-C6)- α(H12-C1-C6)	wag CH_2(C6)
S_{38}	α(H11-C1-C2)+ α(H12-C1-C6)+ α(H11-C1-C6)+ α(H12-C1-C2)	CH_2(C6)
S_{39}	α(H11-C1-C2)+ α(H11-C1-C6)+ α(H12-C1-C2)+ α(H12-C1-C6)	$_wCH_2$(C6)
S_{40}	5 α(H11-C1-H12)+α(C2-C1-C6)	CH_2(C7)
S_{41}	α(H11-C1-C2)+ α(H12-C1-C2)- α(H11-C1-C6)- α(H12-C1-C6)	wag CH_2(C7)
S_{42}	α(H11-C1-C2)+ α(H12-C1-C6)+ α(H11-C1-C6)+ α(H12-C1-C2)	CH_2(C7)
S_{43}	α(H11-C1-C2)+ α(H11-C1-C6)+ α(H12-C1-C2)+ α(H12-C1-C6)	wCH_2(C7)
S_{44}	5 α(H11-C1-H12)+α(C2-C1-C6)	CH_2(C8)
S_{45}	α(H11-C1-C2)+ α(H12-C1-C2)- α(H11-C1-C6)- α(H12-C1-C6)	wag CH_2(C8)
S_{46}	α(H11-C1-C2)+ α(H12-C1-C6)+ α(H11-C1-C6)+ α(H12-C1-C2)	CH_2(C8)
S_{47}	α(H11-C1-C2)+ α(H11-C1-C6)+ α(H12-C1-C2)+ α(H12-C1-C6)	wCH_2(C8)
S_{48}	2α(H24-C9-H23)- α(H23-C9-H25)- α(H25-C9-H24)	aCH_3
S_{49}	α(H23-C9-H25)- α(H25-C9-H24)	aCH3
S_{50}	α(H24-C9-H23)+ α(H23-C9-H25)+ α(H25-C9-H24)- (H25-C9-N3)+ H24-C9-N3)+(H23-C9-N3)	sCH3
S^{51}	2(H25-C9-N3)- H24-C9-N3)-(H23-C9-N3)	CH3
S_{52}	H24-C9-N3)-(H23-C9-N3)	'CH3
S_{53}	(C2-N3-C9-H23)+ (C4-N3-C9-H23)+ (C2-N3-C9-H24)+ (C4-N3-C9-H24)+ (C2-N3-C9-H25)+(C4-N3-C9-H25)	wCH3
S_{54}	2(H13-C2-C1)+ (H13-C2-C8)- (H13-C2-N3)	C2H13
S_{55}	(H13-C2-C8)- (H13-C2-N3)	'C2H13
S_{56}	2(H14-C4-N3)+ (H14-C4-C5)- (H14-C4-C7)	C4H14
S_{57}	(H14-C4-C5)- (H14-C4-C7)	'C4H14
S_{58}	(C9-N3-C4)+ (C9-N3-C2)	N3-C9
S_{59}	(C9-N3-C4-C2)	N3-C9
S_{60}	12-1/2 [2a (C6-C1-C2) - a (C1-C2- C3) - a (C2-C3-C4) + 2a (C3- C4-C5)- a (C4-C5-C6) - a (C5-C6-C1)]	βR2(A1)
S_{61}	½ [a(C4-C5-C6)- a(C1-C2-N3)+ a(C5-C6-C1) - a(C2-N3-C4)]	βR3(A1)
S_{62}	6-1/2 [t (C1-C2- C3-C4) - t (C2-C3-C4-C5) + t (C3- C4-C5-C6) - t (C4-C5-C6-C1) + t (C5-C6-C1-C2) - t (C6-C1-C2-C3)]	R_1(A1)
S_{63}	½ [-t (C3- C4-C5-C6)+ t (C1-C2- C3-C4)- t (C6-C1-C2-C3) + t (C4-C5-C6-C1)]	R_2(A1)
S_{64}	12-1/2 [-t (C1-C2- C3-C4) + 2t (C2-C3-C4-C5) - t(C3- C4-C5-C6) - t (C4-C5-C6-C1) + 2t (C5-C6-C1-C2) - t (C6-C1-C2-C3)]	R_3(A1)
S_{65}	(N3-C4-C7) + a [(C4-C7-C8) + (C2-N3-C4)] + b [(C7-C8-C2) + (C8-C2-N3)]	$βR_1$(A2)
S_{66}	(a-b) [(C4-C7-C8) - (C2-N3-C4)] + (1-a) [(C7-C8-C2) - (C8-C2-N3)]	$βR_2$(A2)
S_{67}	(C7-C8-C2-N3) + b [(N3-C4-C7-C8) + (C2-N3-C4-C7] + a [(C4-C7-C8-C2) + (C8-C2-N3-C4)]	R_1(A2)
S_{68}	(a-b) [(C8-C2-N3-C4) - (C4-C7-C8-C2)] + (1-a) [(C2-N3-C4-C7) - (N3-C4-C7-C8)]	R_2(A2)
S_{69}	2(H26-N3-C9)- (H26-N3-C4)-(H26-N3-C2)	N_3-C9
S_{70}	(H26-N3-C4)-(H26-N3-C2)	'N3-C9
S_{71}	(Cl10-H26-N3)	δCl10-H26-N3
S_{72}	(Cl10-H26-N3-C2)+ (Cl10-H26-N3-C4)+ (Cl10-H26-N3-C9)	$_wH$26-N3

a= cos 144ş, b=cos 72ş

Abbreviations:, stretching; δ deformation in the plane; deformation out of plane; wag, wagging; , torsion; R, deformation ring R, torsion ring; , rocking; twis, twisting; , angular deformation;

, deformation; a, antisymmetric; s, symmetric; A_1, Ring 1 (piperidine); A_2, Ring 2 (pyrrolidine) coupled with deformation or rocking modes between 1478 and 1400 cm-1 and, for this reason, those two modes in the three species are assigned, as indicated in Table 3. On the other hand, the rocking modes are predicted between 1183 and 1128 cm-1 while the twisting modes between 205 and 151 cm-1 and, for these reasons, in each species those modes were assigned according to SQM calculations. These CH_3 vibration modes in nitrogen species derived from tricyclic bisguanidine compound [32] and in N-benzylamides [48] are assigned in the same regions.

CH_2 modes. The three tropane species have each five CH_2 groups for which are expected ten antisymmetric and symmetric stretching modes and five deformation, wagging, rocking and twisting modes. The two stretching modes are predicted between 3024 and 2911 cm-1, the deformation modes between 1485 and 1442 cm-1, the wagging modes between 1385 and 1274 cm-1, the rocking modes between 1274 and 1142 cm-1 and the twisting modes between 967 and 639 cm-1. In some of the three species, all these modes appear strongly coupled among them, as observed in Table 3. This way, they were assigned according to SQM calculations and in the same regions expected for compounds containing that CH_2 group [32,47,48,50].

Skeletal modes. The three IR bands, one with medium intensity and the other two very intense, at 1128, 1086 and 1031 cm-1 are clearly assigned to the N-CH3 stretching modes of the neutral, hydrochloride and cationic species, respectively because the SQM calculations predicted those modes at 1141, 1085 and 1029 cm-1, as observed in Table 3. The two N-C stretching modes corresponding to both rings are predicted in different regions, thus, in the hydrochloride species those modes are predicted at 761 and 710 cm-1, in the cationic species at 733 and 673 cm-1 while in the neutral species at 998 and 750 cm-1. Then, the IR bands at 981, 776, 729, 706 and 680 cm-1 are easily assigned to those vibration modes of the three tropane species. In relation to the six and five member's ring (see Fig. 3), these are formed by the fused piperidine and pyrrolidine rings. In the first case, we expected three deformations which are, βR1(A1), βR2(A1) and βR3(A1) and three torsion rings (R1, R2 and R3) while in the second one only two deformations (βR1(A2), βR2(A2)) and two torsion rings (R1 and R2) are expected. Here, the redundant internal coordinates was identified as βR1(A1) for which, it was removed. In general, we observed that these modes are strongly mixed among them, as can be seen in Table 3. The assignments of these modes was performed according to the SQM calculations and taking into account those reported for species with similar rings [32,47-51]. Remain skeletal modes can not be assigned because the IR spectra only was recorded in the 4000-680 cm-1 region.

FORCE CONSTANTS

The force fields for those three tropane species expressed in Cartesian coordinates by using the B3LYP/6-31G* method were computed with the SQMFF approach [29] and the Molvib program [42]. Later, those force fields transformed to internal coordinates were used to calculate the force constants at the same level of theory. Table 5 shows a comparison of those main scaled internal force constants for the neutral, cationic and hydrochloride tropane species in gas and aqueous solution phases with those reported for cyclic nitrogen species structurally associated to the tricyclic bisguanidine compound in gas phase at the same level of theory [32]. Comparing first the values for the tropane forms, we observed that the *f(vN-H)* constant in gas phase for the cationic species is higher than the corresponding to hydrochloride, as expected because the predicted N-H distance in the cationic form is 1.025 A while in the other one the distance is 1.135 A. Hence, that geometrical parameter justifies the higher value in the cationic species. In solution, the value increase for the hydrochloride species while remains practically constant for the cationic form. Hence, in general all force constants increase in the cationic forms because this species is strongly hydrated in solution, this species presents higher solvation energy and, as a consequence this species undergoes a volume contraction in this media where we observed decreasing in the C-C, N-C and N-CH_3 distances and bond angles, as was analyzed in section 3.2. On the contrary, in the hydrochloride species we observed increase in the *f(vN-H)* constant but a decreasing in the *f(N-CH_3)* and *f(C-N)* constants which can be attributed to the N-CH_3 and C-N distances values because these parameters increase in solution, as observed in **Table 2**.

TABLE – 5

Comparison of main scaled internal force constants for the neutral, cationic and hydrochloride tropane forms in gas and aqueous solution phases compared with those reported for cyclic nitrogen species.

B3LYP/6-31G*									
Force constant	Tropane[a]						Tricyclic[b] bisguanidine		STX[b]
	Neutral		Cationic		Hydrochloride		Cyclic		
	Gas	PCM	Gas	PCM	Gas	PCM	CN	CC	
f(N-H)			5.97	5.98	2.70	4.69	6.46	6.67	6.00
f(N-CH_3)	4.69	4.52	4.09	4.21	4.42	4.26			
f(C-N)	4.16	3.97	3.11	3.35	3.73	3.48	5.00	4.12	4.42
f(CH_2)	4.78	4.78	4.88	4.88	4.85	4.87	4.83	4.91	4.93
f(CH_3)	4.72	4.79	5.10	5.13	5.03	5.11	4.85	4.91	
f(C-H)	4.78	4.82	4.92	4.99	4.90	4.96			
f(C-C)	4.05	4.06	4.17	4.21	4.16	4.20	3.87	3.78	3.87
f(CH_2)	0.74	0.72	0.75	0.72	0.74	0.73	0.76	0.75	0.76
f(CH_3)	0.58	0.57	0.56	0.56	0.56	0.56	0.56	0.56	

Units are mdyn A-1 for stretching and mdyn A rad-2 for angle deformations [a]This work, [b]From Ref. [32]

For the neutral species, the *f(v N-CH_3)* and *f(v C-N)* constants decrease in solution according increase the respective distances in this medium. Comparing the values of the three species with those reported for the cyclic nitrogen species and saxitoxin [32], we observed that the higher f(*v*N-H) values are calculated for those cyclic compounds. The differences could be justified probably because the N atoms belong to the N-H groups have sp^2 hybridization while in the tropane species the N atoms present sp^3 hybridization. This means that in the cyclic species the N-H atoms are in a plane while in the tropane species there is a tertiary nitrogen atom where the N-H group is in a tetrahedron and not planar, as in the cyclic species.

CONCLUSIONS

The most important results of this work are the following:

- The cationic, neutral and hydrochloride structures of tropane species were theoretically determined in gas and aqueous solution phase by using the B3LYP/6-31G* method while the solvation energies for those three species were predicted by using the SCRF/PCM/SMD methods.
- Our results confirm the fast N-methyl inversion in gas phase and in aqueous solution for the cationic and hydrochloride species in relation to the neutral species at room temperature, as reported in the literature.
- The force fields for those three species in both media were obtained at the same level of theory by using the SQMFF procedure and the complete assignments of the 66, 69 and 72 vibration normal modes expected for the neutral, cationic and hydrochloride tropane species, respectively are reported for first time.
- The normal internal coordinates for all species were employed to compute the corresponding force fields where, in particular, for the bicyclic (N-methyl-8-a-zabicyclo[3.2.10]octane) group was considered as formed by two fused piperidine and pyrrolidine rings, six and five member's rings, respectively. The redundant internal coordinates due to the C-N-C group shared by both rings was identified and then, removed from the corresponding force fields.
- The tropane hydrochloride in solid state is in their cationic form, as expected because it is a salt and, besides, the corresponding predicted IR spectrum for this species is in very good agreement with the experimental one.

- The identifications of all the normal internal coordinates are very important for the elucidation of all the tropane alkaloids and their derivatives, because these results will be used in a future to perform the force fields for other alkaloids, such as scopolamine or atropine and, on the other hand, with the assignments reported here it is possible the detection of these important alkaloids by using vibrational spectroscopy.

ACKNOWLEDGEMENTS

This work was supported with grants from CIUNT Project Nº 26/D207 (Consejo de Investigaciones, Universidad Nacional de Tucumán). The authors would like to thank Prof. Tom Sundius for his permission to use MOLVIB.

REFERENCES:

[1] Buckett, W.R.; Haining, C.G. (1965). Some pharmacological studies on the optically active isomers of hyoscine and hyoscyamine, Brit. J. Pharmacol., 24, 138-146.
[2] Mandava, N.; Fodor, G. (1968). Configuration of the ring nitrogen in N-oxides and the conformation of tropanes. Part XVIII, Canad. J. Chem. 46(17), 2761-2766.
[3] Weinstein, H.; Srebrenik, S.; Maayani, S.; Sokolovsk, M. (1977). A Theoretical Model Study of the Comparative Effectiveness of Atropine and Scopolamine Action in the Central Nervous System, J. Theor. Biol. 64, 295-309.
[4] a-Feeney, J. Foster, R.; Piper, E. A. (1977) J. Chem. Soc., Perkin Trans. 2, 201 (6). b-Weiler, E.W.; Stockigt, J.; Zenk, M.H. (1981). Radioimmunoassay for the quantitative determination of scopolamine, Phytochemistry, 20(8), 2009-2016.
[5] Cantor, E.H.; Abraham, S.; Marcum, E.A.; Spector, S. (1983). Structure-activity requirements for hypotension and et-adrenergic receptor blockade by analogues of atropine, European Journal of Pharmacology, 9075-83.
[6] Hammon, K.; De Martino, B. (1985) Postoperative Delirium Secondary to Atropine Premedication, Anesthesia Progress, 107-108.
[7] Armstrong, D.W.; Han, S.M.; Han, Y.I. (1987). Separation of Optical Isomers of Scopolamine, Cocaine, Homatropine, and Atropine, Analytical Biochemistry 167, 261-264.
[8] Sarazin, C.; Goethals, G.; Séguin, J-P.; Barbotin, J-N. (1991). Spectral reassignment and structure elucidation of scopolamine free base through two-dimensional NMR techniques, Magnetic Resonance in Chemistry 29(4), 291-300.
[9] Fliniaux, M-A.; Manceau, F.; Dubreuil, A.J. (1993). Simultaneous analysis of l-hyoscyamine , Z-scopolamine and &tropic acid in plant material by reversed-phase high-performance liquid chromatography, Journal of Chromatography, 644, 193-197.
[10] Glaser, R.; Shiftan, D.; Drouin, M. (2000). The solid-state structures of (-)-scopolamine free base, (-)-scopolamine methobromide, (-)-scopolamine hydrobromide trihydrate, and of the pseudopolymorphic forms of (-)-scopolamine hydrochloride anhydrate and 1.66 hydrate, Canadian Journal of Chemistry, 78(2), 212-223.
[11] Niu, Y-Y; Yang, L-M; Liu, H-Z; Cui, Y-Y; Zhu, L.; Feng, J-M; Yao, J-H; Chen, H-Z; Fan, B-T; Chen, Z-N; Lu, Y. (2005). Activity and QSAR study of baogongteng A and its derivatives as muscarinic agonists, Bioorganic & Medicinal Chemistry Letters 15, 4814–4818
[12] Xiang, X-H; Wang, H-L; Wu, W-R; Guo, Y; Cao, D-Y; Wang, H-S; Zhao, Y. (2006). Ethological analysis of scopolamine treatment or pretreatment in morphine dependent rats, Physiology & Behavior 88 ,183–190.
[13] De Simone, R.; Margarucci, L.; De Feo, V. (2008). Tropane alkaloids: An overview, Pharmacologyonline 1, 70-89.
[14] Beyer, J.; Drummer, O.H.; Maurer, H.H. (2009). Analysis of toxic alkaloids in body samples, Forensic Science International 185, 1–9.
[15] Klinkenberg, I.; Blokland, A. (2010). The validity of scopolamine as a pharmacological model for cognitive impairment: A review of animal behavioral studies, Neuroscience and Biobehavioral Reviews 34, 1307–1350.
[16] Ricard, F.; Abe, E.; Duverneuil-Mayer, C.; Charlier, P.; de la Grandmaison, G.; Alvarez, J.C. (2012). Measurement of atropine and scopolamine in hair by LC–MS/MS after Datura stramonium chronic exposure, Forensic Science International 223, 256–260.
[17] Wang, J-H.; Chena, Y-M.; Carlson, S.; Li, L.; Hu, X-T.; Ma, Y-Y. (2012) Interactive effects of morphine and scopolamine, MK-801, propanolol on spatial working memory in rhesus monkeys, Neuroscience Letters 523, 119– 124.
[18] Veeranjaneyulu, P.; Rao, T.B.; Mantha, S.; Vaidyanathan, G.A. (2012)sensitive method for the estimation of scopolamine um human plasma using ACQUITY UPLC and Xevo TQ-S, Waters Corporation, Bangalore, India, 1-7.
[19] Alhaider, I. A. (2013). Effects of edaravone and Scopolamine induced-dementia in experimental rats, Int. J. Pharmacology, 9(4), 271-276.
[20] Ma, L.; Gu, R.; Tang, L.; Chen, Z-E; Di, R.; Long, C. (2015). Important Poisonous Plants in Tibetan Ethnomedicine, Toxins, 7, 138-155.
[21] Sweta, V.R.; Lakshmi, T. (2015). Pharmacological profile of tropane alkaloids, Journal of Chemical and Pharmaceutical Research,, 7(5):117-119.
[22] García-Ruiz, C.; Sáiz, J. (2014). Reply to Letter to the Editor, In response to the letter "Scopolamine: Useful medicine or dangerous drug? Science and Justice 54, 323.
[23] Pauling, P.; Datta, N. (1980). Anticholinergic substances: A single consistent conformation, Proc. Natl. Acad. Sci. 77(2), 708-712.
[24] Lazny, R.; Ratkiewicz, A.; Nodzewska, A.; Wynimko, A.; Siergiejczyk, L. (2012). Determination of the N-methyl stereochemistry in tropane and granatane derivatives in solution: a computational and NMR spectroscopic study, Tetrahedron Letters.
[25] Barbat, C.; Rodino, S.; Petrache, Butu, P.M.; Butnariu, M. (2013) Microencapsulation of the allelochemical compounds and study of their release from different products, Digest Journal of Nanomaterials and Biostructures 8(3), 945-953.
[26] a- Hui , G Zhao, Y Zhang , W Xie, YF Yang , JX Zhao , DQ Zhao, B. (2010). Raman spectroscopy study on the interaction of ginsenoside Rb1 with DPPC bilayers, 30(9), 2393-2396.
[27] Zhao, B.; Li, X.; Zhao, D.; Ni, J. Chen, J.; Hwang, F. (1998). Interaction of Scopolamine and Cholesterol with Sphingomyelin Bilayers by FT-Raman Spectroscopy, Spectroscopy Letters 31(8), 1825-1837.
[28] Gyermek, L. The role of the tropane skeleton in drug research, was presented as a lecture in Hungarian, on the occasion of his election as Foreign Member of the Hungarian Academy of Medical Sciences (Division V-Medical Sciences), September, (2005).
[29] a) Rauhut, G.; Pulay, P. (1995). J. Phys. Chem. 99 3093-3099. b) Correction: G. Rauhut, P. Pulay, J. Phys. Chem. 99 (1995) 14572.
[30] Becke, A.D. (1988). Density-functional exchange-energy approximation with correct asymptotic behavior, Phys. Rev., A38, 3098-3100.
[31] Lee, C.; Yang, W.; Parr. R.G. (1988). Development of the Colle-Salvetti correlation-energy formula into a functional of the electron density, Phys. Rev. B37, 785-789.
[32] Romani, D.; Tsuchiya, S.; Yotsu-Yamashita, M.; Brandán, S.A. (2016). Spectroscopic and structural investigation on intermediates species structurally associated to the tricyclic bisguanidine compound and to the toxic agent, saxitoxin, J. Mol. Struct. 1119, 25-38.
[33] Nielsen, A.B.; Holder, A.J. Gauss View 3.0, User's Reference, GAUSSIAN Inc., Pittsburgh, PA, 2000–2003.
[34] Frisch, M.J. et al., GAUSSIAN 09, Revision A.02, Gaussian, Inc., Wallingford, CT, 2009.
[35] Hamor, T.A.; Kings, N. (1980). Structure of 3□-Bromotropane Hydrobromide Monohydrate, Acta Cryst.. B36, 3153-3155.
[36] Bode, J.; Stam, C. H. (1982). The Absolute Configuration of the Tropane Alkaloid 6□,7□-Epoxy-l□H,5□H~tropan-3□-yl(-)-2,3-Dihydroxy-2-phenylpropionate from its n-Butylbromide, Acta Cryst. B38, 333-335.
[37] Muñoz, M.A.; Muñoz, O.; Joseph-Nathan, P. (2010). Absolute Configuration Determination and Conformational Analysis of (2)-(3S,6S)-3a,6b-Diacetoxytropane Using Vibrational Circular Dichroism and DFT Techniques, Chirality 22, 234–241.
[38] Tomasi, J. Persico, J. (1994). Molecular Interactions in Solution: An Overview of Methods Based on Continous Distributions of the Solvent, Chem. Rev. 94, 2027-2094.
[39] Miertus, S.; Scrocco, E.; Tomasi, J. (1981). Electrostatic interaction of a solute with a continuum. Chem. Phys. 55, 117–129.
[40] Marenich, A.V.; Cramer, C.J.; Truhlar, D.G. (2009). Universal solvation model based on solute electron density and a continuum model of the solvent defined by the bulk dielectric constant and atomic surface tensions, J. Phys. Chem. B113, 6378-6396.
[41] Ugliengo, P. MOLDRAW Program, University of Torino, Dipartimento Chimica IFM, Torino, Italy, 1998.
[42] Sundius, T. (2002). Scaling of ab initio force fields by MOLVIB, Vib. Spectrosc. 29, 89-95.
[43] Pulay, P.; Fogarasi, G.; Pang, F.; Boggs, J.E. (1979). Sistematic ab Initio gradient calculation of molecular geometries, force constants and dipole moment derivatives, J. Am. Chem. Soc. 101(10), 2550-2559.
[44] Infrared spectrum, http://webbook.nist.gov/cgi/inchi?ID=C23555068&Mask=80.
[45] Keresztury, G.; Holly, S.; Besenyei, G.; Varga, J.; Wang, A.Y.; Durig, J.R. (1993). Vibrational spectra of monothiocarbamates-II. IR and Raman spectra, vibrational assignment, conformational analysis and ab initio calculations of S-methyl-N,N-dimethylthiocarbamate Spectrochim. Acta, 49A, 2007-2026.
[46] Michalska, D.; Wysokinski, R. (2005). The prediction of Raman spectra of platinum(II) anticancer drugs by density functional theory, Chemical Physics Letters, 403.
[47] Romano, E.; Davies, L.; Brandán, S.A. (2017). Structural properties and FTIR-Raman spectra of the anti-hypertensive clonidine hydrochloride agent and their dimeric species, J. Mol. Struct. 1133, 226-235.
[48] Chain, F.E.; Ladetto, M.F.; Grau, A.; Catalán, C.A.N.; Brandán, S.A. (2016). Structural, electronic, topological and vibrational properties of a series of N-benzylamides derived from Maca (Lepidium meyenii) combining spectroscopic studies with ONION calculations, J. Mol. Struct. 1105, 403-414.
[49] Márquez, M.J.; Márquez, M.B.; Cataldo, P.G.; Brandán, S.A. (2015). A comparative study on the structural and vibrational properties of two cyanopyridine derivatives with potentials antimicrobial and anticancer activities, Open Journal of Synthesis Theory and Applications, 4, 1-19.
[50] Márquez, M.B.; Brandán, S.A. (2014). A structural and vibrational investigation on the antiviral deoxyribonucleoside thymidine agent in gas and aqueous solution phases, Int. J. Quantum Chem. 114, 209-221.
[51] Cataldo, P.G.; Castillo, M.V.; Brandán, S.A. (2014). Quantum mechanical modeling of fluoromethylated-pyrrol derivatives. A study on their reactivities, structures and vibrational properties, Phys Chem Biophys, 4(1), 4-9.
[52] Brizuela, A.B.; Raschi, A.B.; Castillo, M.V.; Leyton, P. Romano, E. Brandán, S.A. (2013). Theoretical structural and vibrational properties of the artificial sweetener sucralose, Comp. Theor. Chem. 1008, 52–60.
[53] Romani, D.; Brandán, S.A. (2015). Structural and spectroscopic studies of two 1,3-benzothiazole tautomers with potential antimicrobial activity in different media. Prediction of their reactivities, Comp. Theor